

archives  
of thermodynamics

Vol. 40(2019), No. 3, 83–108

DOI: 10.24425/ather.2019.129995

## Experimental study of the prototype of a Roto-Jet pump for the domestic ORC power plant

TOMASZ Z. KACZMARCZYK<sup>1\*</sup>  
EUGENIUSZ IHNATOWICZ<sup>1</sup>  
GRZEGORZ ŻYWICA<sup>1</sup>  
MACIEJ KANIECKI<sup>2</sup>

<sup>1</sup> Institute of Fluid Flow Machinery, Polish Academy of Sciences  
Department of Turbine Dynamics and Diagnostics, Fiszerza 14,  
80-231 Gdańsk

<sup>2</sup> ZRE Gdańsk S.A., Litewska 14a, 80-719 Gdańsk

**Abstract** The purpose of the work was to experimentally determine the characteristics of the prototype of a Roto-Jet pump (the Pitot tube pump) during its operation under conditions typical for the domestic micro power plant. The low-boiling fluid, sold under the trade name of HFE7100 and characterised by a zero ozone depletion potential (ODP) coefficient, was used as a working medium in the organic Rankine cycle (ORC). An electric thermal oil heater with a maximum power of  $2 \times 24 \text{ kW}_e$  was used as a heat source. The pump of Roto-Jet type was specially designed for the operation with the following rated parameters of the thermodynamic cycle: nominal flow rate of the working fluid  $0.17 \text{ kg/s}$ , operating pressure  $1.2 \text{ MPa}$ . The pump was put under load using an expansion valve that simulated the operation of an expansion machine. The article discusses thermodynamic and flow conditions to be met by the pumping engine as well as results of the experimental research. Moreover, the article includes the operational characteristics of the ORC installation and the Roto-Jet pump obtained during the operation with the target working medium – HFE7100. The engineering problems the authors of this article faced when designing and testing the pumping engine prototype are also presented.

---

\*Corresponding Author. Email: tkaczmarczyk@imp.gda.pl

**Keywords:** Roto-Jet pump; Pitot tube pump; Domestic ORC micropower plant; Low-boiling medium

## Nomenclature

$a$	–	total coefficient of flow losses inside the Roto-Jet pump's channel
$A$	–	inlet area of the pump impeller, $\text{m}^2$
$f$	–	cross-sectional area of the Roto-Jet pump's inlet, $\text{m}^2$
$g$	–	gravitational acceleration, $\text{m/s}^2$
$H$	–	actual head of the Roto-Jet pump, m
$H_t$	–	theoretical delivery head of the impeller, m
$h_{wb}$	–	flow losses in the rotary drum, m
$K_H$	–	head coefficient dependent on the vena contraction of the Roto-Jet pump
$n_{sQ}$	–	specific shape
$p$	–	pressure, Pa
$p_{wb}$	–	liquid pressure at the rotary drum's inlet, Pa
$p_{wd}$	–	liquid pressure at the diffuser inlet, Pa
$t$	–	temperature
$Q$	–	volumetric flow rate of the working medium, $\text{m}^3/\text{s}$
$r_s$	–	average radius of the cross-sectional area of the Roto-Jet pump's inlet, m
$u_z$	–	drift velocity on the outer contour of the impeller, m/s
$v_{wb}$	–	liquid velocity at the rotary drum's inlet, m/s
$v_{wc}$	–	liquid velocity at the Roto-Jet pump's inlet, m/s
$v_{wd}$	–	liquid velocity at the diffuser inlet, m/s
$x$	–	quality

## Greek symbols

$\xi_{wc}$	–	coefficient of flow losses at the bucket inlet
$\xi_{wd}$	–	coefficient of flow losses at the diffuser inlet
$\omega$	–	angular velocity of the rotating liquid, rad/s
$\omega_k$	–	angular velocity of the impeller, rad/s
$\varphi$	–	specific performance indicator
$\psi$	–	specific delivery head indicator

## Abbreviation

ORC	–	organic Rankine cycle
CHP	–	combined heat and power
ODP	–	ozone depletion potential
BWR	–	back work ratio
NPSH	–	net positive suction head
NPSHR	–	net positive suction head required

## 1 Introduction

The development and commercialisation of small ORC systems are limited by the lack of circulation pumps for the working fluid, which can be di-

rectly applied in these systems [1]. In small ORC systems, a low flow rate at a high forcing pressure of the working fluid is required. The efficiency of such systems ranges from 7% to 25% [2]. Low critical temperatures of the working fluids in subcritical organic Rankine cycles (ORCs) cause that pumps consume significant quantities of energy (i.e., from 11% to 30% of electricity produced by expansion machines) [3,4]. There are many varieties of small combined heat and power (CHP) cycles, which can differ from each other in terms of heat sources, working fluids and/or expansion machines used in them. However, commercial pumps are often not capable of achieving appropriate operating parameters so as to use them in small ORCs [5].

For example, positive displacement pumps (i.e., piston, screw and scroll pumps) trigger flow and pressure pulsations [1]. Their operation is accompanied with high noise levels and there are some limitations related to the viscosity of working fluids. Such pumps cannot function with low viscosity liquids. What is more, they must have high manufacturing accuracy, which translates into their high purchase price and high maintenance costs associated with exchanging of friction pairs. However, with low values of the specific speed in conventional single-stage pumps, there are large power losses due to the friction of rotor discs and also low efficiencies as well as major leakages in the immediate vicinity of ring seals. Multistage pumps have more complex constructions and their purchase and maintenance costs are higher [6,7]. However, one has to bear in mind that the suction pipeline must be properly designed and suitable fittings should be used in order to avoid an excessive vibration level of the pumping engine (which could result in failure of the pump). The pressure inside the pump falls as the flow rate of the working fluid rises, which can have various negative effects such as cavitation, increased noise and vibration levels, erosion, faster wear of bearings or a shorter life of the pumping engine (even up to 20 times). In order to prevent these effects, it is recommended to use an appropriate length of the pump's suction pipeline as well as the appropriate flow rate of the working medium, what ensures optimal vibration level of the pump [8–11].

On the basis of information found in literature [12,13] it can be said that even if net positive suction head required (NPSHR) criteria are met, a liquid recirculation can occur in the pumping system, which will reduce the effective cross-sectional area of the pipeline at the suction inlet and also will cause the liquid velocity field to become non-uniform. This phenomenon is manifested in the appearance of an excessive flow rate of the

working liquid, an excessive vibration level, higher power consumption of the pump and cavitation. Consequently, they all can shorten the pump's life by about 58% in relation to the nominal value. Therefore, in the industrial pump systems operated for a longer period of time, numerical analyses are carried out to ensure the value of the NPSH (net positive suction head) coefficient is optimal while maintaining the nominal efficiency of the pump [14].

It should be noted that most commercial pumps are dedicated to a specific industry and a specific liquid. In low power ORC cogeneration systems many very different working fluids of various viscosities are used. Such systems are required to have high efficiency, low power consumption, low purchase price, and additionally, should be reliable and very durable. The use of a commercial pump in an ORC system is often associated with its operation in a non-optimum regime [15].

Roto-Jet pumps (Pitot tube pumps or rotary drum pumps) [16], which enable operation at low rotational speeds, are an interesting alternative to the above-mentioned pumps. Such pumps are characterized by a simple construction, operational reliability and are simple to use. In comparison to a conventional rotodynamic pump, a Pitot tube pump has an approximately 1.6 times higher delivery head at the same specific speed and pump size but its purchase cost is lower. Furthermore, such a pump can produce high pressure at a low rotational speed (even if it is a single-stage pump) [17]. For instance, pumps with a capacity of 1.8–2.2 m<sup>3</sup>/h have a delivery head of approximately 100 m, which is achieved at a rotational speed of approx. 2900 rpm [18,19]. On the other hand, Roto-Jet pumps are used in various industrial sectors, such as food industry, paper industry, power engineering (used as injection pumps for NO<sub>x</sub> control in gas turbines) or in refineries as well as industrial boiler systems and petrochemical systems. Moreover, they are used in automobile industry, mining industry, reverse osmosis process [17], and even in ORC systems using low-boiling fluids [20]. Nowadays, Pitot tube pumps [21,22] are observed to develop fast owing to their advantages such as low purchase cost, high reliability, simplicity of design, high delivery head at low flow rates of working fluids and great potential of applications in various sectors of industry. Since both website and the scientific literature provide only basic information on Roto-Jet pumps, it was necessary to conduct experimental research and numerical analyses of circulation pumps operating in ORCs.

For instance, Lei *et al.* [1] simulated operation of a Roto-Jet pump in an

ORC at various rotational speeds. They analyzed the ORC with R123 and R245fa working fluids. They observed that an increase in the rotational speed of the pump had a greater effect on the gain in forcing pressure than the increase in the flow rate of the working fluid. They found that the efficiency of the pump decreased (which ranged from 11% to 23%) as its rotational speed increased and the flow rate of the working fluid decreased. On the other hand, an increase in the forcing pressure of the pump caused a drop in the flow rate, which stems from larger pump leaks as a result of the increase in differential pressure between the suction and discharge ports and the low viscosity of the working liquids. Moreover, the work and power absorbed by the pump increase (above the values visible on theoretical curves) as the evaporation temperature of the working fluid rises, which is caused by a decrease in the efficiency of the pump. The authors found that the efficiency of the ORC increased from 5.9% to 7.9% as the rotational frequency of the pump rose from 40 Hz to 70 Hz. They have concluded that the value of the back work ratio (BWR) decreased and the efficiency of the ORC increased as the overheating degree of the working fluid increased.

The results of the research carried out by Meyer *et al.* [6,7] show that the poorly designed geometry of the delivery channel of the pump's blade system can cause the internal losses of the pump to increase by up to 55% compared to the nominal operating point. The authors claim that it is possible to decrease the losses inside the pump by about 70% by applying an appropriate optimization algorithm. In addition, the use of a permanent magnet brushless direct current (BLDC) motor for the construction of a pumping engine with a Pitot tube pumps reduces the overall size of the entire assembly by about 40% compared to conventional units and eliminates gears and couplings [23].

Komaki *et al.* [24] conducted a numerical analysis and experimental research of a pump with a Pitot tube pump, which was used for feeding the boiler. They determined that the efficiency of the pump and its delivery head are both affected not only by the efficiency of the diffuser but also by the external profile of the flow system as well as the flow rate and dynamic pressure of the rotary body. In addition, they observed that the capacity of the pump worsened as its rotational speed increased. Zhu *et al.* [25] performed a numerical analysis of various geometries of a Pitot tube pump and the collector of a pump in terms of energy efficiency. The nominal operating parameters of the pump were as follows: a capacity of 7.2 m<sup>3</sup>/h

and a delivery head of 168 m at a speed of 3550 rpm. Based on the numerical analysis, they determined that the flow rate dropped at the inlet to the Pitot tube of the pump, which resulted in the increase in total static pressure and its uneven distribution in the collector. They determined that the use of the wheel in the pump's feed system reduces hydraulic forces and eliminates pressure fluctuations in the pump.

## 2 Test ring

The research on a prototypical Roto-Jet pump of the PCz 95.7 type was conducted during its operation in a prototypical ORC micro-cogeneration power plant with an electric power of 3 kW<sub>e</sub>, which was constructed under project No. POIG.01.01.02-00-016/08, entitled 'Model agroenergy complexes as an example of distributed cogeneration based on local and renewable sources of energy'. The test rig consists of three main cycles of working fluids. The first cycle is a heating cycle and consists of a heat source, circulation pump, heat exchanger (evaporator), pipelines as well as control and measurement fittings. An electric heater that comprises two modules, each of which has an electric power of 24 kW<sub>e</sub>, was used as a heat source in the system. This heater served for heating the heat-transfer fluid (thermal oil), which was then used to heat the working fluid (HFE7100). The second cycle, namely the working fluid cycle, consists of an expansion valve (which simulates operation of an expansion machine), heat exchangers (regenerator and condenser), working fluid tank, circulation pump (the Roto-Jet pump that was subjected to research), droplet separator for the working fluid vapor, evaporator, pipelines as well as control and measurement apparatus. The ORC installation can operate either with or without regeneration, as the schemes in Figs. 1 and 2 show.

The third cycle is a cooling cycle and consists of a fan cooler with a power rating of 50 kW<sub>t</sub>, condenser, pump for the cooling medium (propylene glycol), fittings as well as control and measurement apparatus. Loading the tested pump was done using an expansion valve that simulated operation of the expansion machine (e.g., a turbine).

### 2.1 Prototypical Rotor-Jet pump

As mentioned before, the circulation pump for the working fluid is one of the main components of the investigated ORC system. This pump must

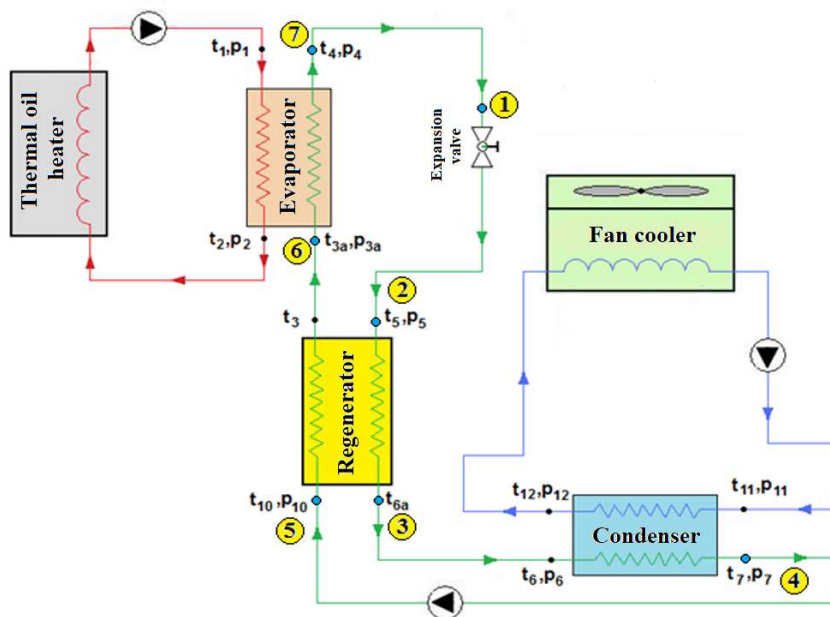


Figure 1: Measurement scheme of the organic Rankine cycle with regeneration.

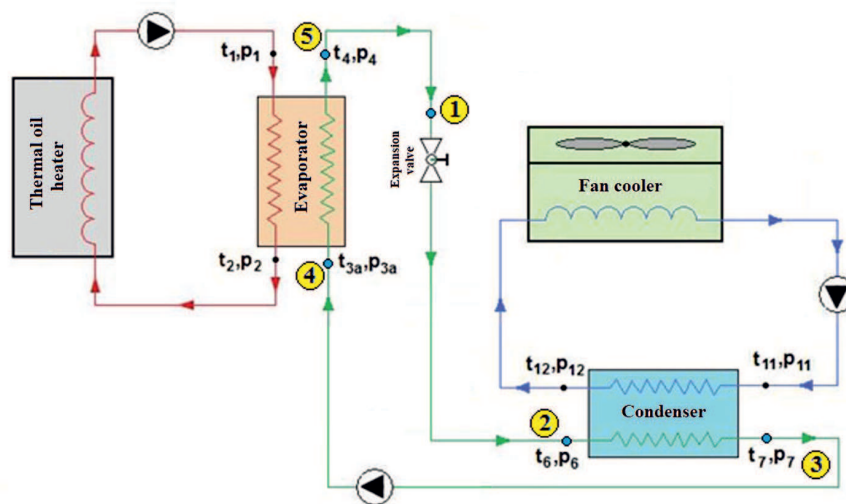


Figure 2: Measurement scheme of the organic Rankine cycle without regeneration.

be able to provide adequate pressure (1.2 MPa absolute pressure) and flow rate (0.17 kg/s) of the working fluid (HFE7100) at the inlet to an expansion machine. Based on the market analysis and measurements made [5], it was found that pumps that meet the above-mentioned criteria are not available. It should be noted that the HFE7100 fluid is a solvent, which considerably limits the possibility of using commercial pumps because of the potential damage to seals and structural elements of the pump (such as, for instance, shaft, bearings, impeller or body). Selected properties of the HFE7100 fluid are listed in Tab. 1.

Table 1: Selected physicochemical properties of the HFE7100 fluid.

Parameter	Value	Unit
Molar mass	250	kg/kmol
Boiling point (at 101.325 kPa)	61	°C
Solidification point (at 101.325 kPa)	-135	°C
Density (at 25 °C)	1520	kg/m <sup>3</sup>
Surface tension (at 25 °C)	13.6	mN/m
Dynamic viscosity (at 25 °C)	0.61	mPa s

It became evident that there was a need to design and manufacture a pump that would not only meet the above operating parameters but exhibit adequate chemical and temperature resistance (the nominal operating temperature is about 65 °C).

Due to the low value of the flow rate in relation to the pressure of the working fluid, it was decided to construct a Roto-Jet pump in a non-symmetrical arrangement, i.e., with one Pitot tube (Fig. 3). Directions of the flow of the working liquid are designated by ‘Q’ in Fig. 3. Streamlines and tip vortices are also shown in this figure.

For the calculation purposes of the pump, it was assumed that the nominal volumetric flow rate of the working fluid is 0.4333 m<sup>3</sup>/h. It should be noted that different sources of information give different values (at a temperature of 65 °C) for the density and viscosity of the HFE7100 liquid and they differ by approx. 4.5% and 8%, respectively [5].

Assuming that the rotary body of the Roto-Jet pump’s drum with radial blades behaves like a flat impeller, the theoretical head of this pump’s



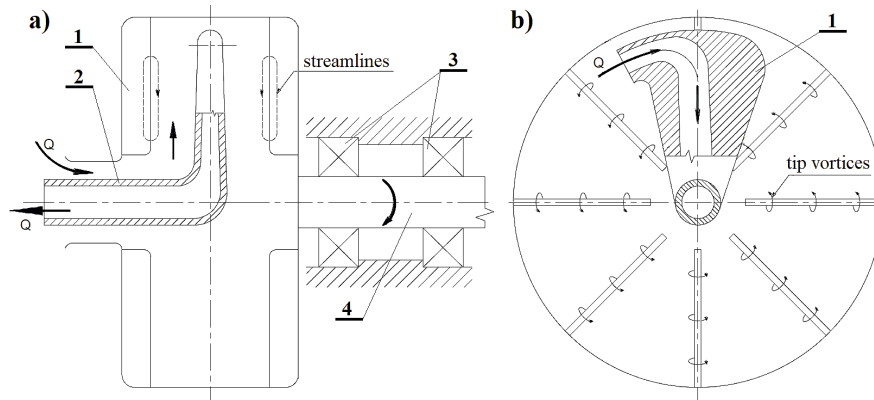


Figure 3: HFE7100 flow diagram inside the Roto-Jet pump of the PCz 95.7 type [26]:  
 a) longitudinal section; b) cross-section; 1 – body, 2 – Pitot tube, 3 – bearing system, 4 – shaft.

rotor can be calculated using the Euler equation, in the following form:

$$H_t = \frac{\omega_k \omega r_s^2}{g}, \quad (1)$$

where:  $\omega_k$  – angular speed of the impeller,  $\omega$  – angular velocity of the rotating liquid,  $r_s$  – average radius of the cross-sectional area of the roto-jet inlet,  $g$  – gravitational acceleration.

The actual delivery head of the pump can be calculated on the basis of the Bernoulli equation, which takes the following form for the stream in the Roto-Jet pump's channel:

$$\frac{p_{wb}}{\gamma} + \frac{v_{wb}^2}{2g} + H_t = \frac{p_{wd}}{\gamma} + \frac{v_{wd}^2}{2g} + \xi_{wc} \frac{v_{wc}^2}{2g} + \xi_{wd} \frac{v_{wd}^2}{2g} + h_{wb}, \quad (2)$$

where:  $p_{wb}$  and  $v_{wb}$  – pressure and velocity of the liquid at the rotary drum's inlet,  $p_{wd}$  and  $v_{wd}$  – pressure and velocity of the liquid at the diffuser inlet,  $v_{wc}$  – liquid velocity at the Roto-Jet pump's inlet,  $\xi_{wc}$  and  $\xi_{wd}$  – coefficient of flow losses respectively at the bucket's and diffuser's inlet,  $h_{wb}$  – flow losses in the rotary drum resulting from the difference in the drum's and liquid's velocity.

Thus, the actual delivery head of the Roto-Jet pump can be calculated by the following formula:

$$H = K_H \frac{(\omega r_s)^2}{g} - \frac{aQ^2}{2gf^2}, \quad (3)$$

where:  $K_H$  – delivery head coefficient dependent on the vena contraction of the Roto-Jet pump,  $a$  – total coefficient of the flow losses inside the bucket channel,  $f$  – the cross-sectional area of the bucket inlet.

For comparative purposes and also to determine the applicability of a given type of pump to the given operating conditions, the following indicators are used: specific shape ( $n_s$ ), specific head indicator ( $\psi$ ) and specific performance indicator ( $\varphi$ ). They can be defined using the following formulas:

$$n_{sQ} = \frac{nQ^{\frac{1}{2}}}{H^{\frac{3}{4}}}, \quad (4)$$

$$\psi = \frac{2gH}{u_z^2}, \quad (5)$$

$$\varphi = \frac{Q}{Au_z}, \quad (6)$$

where:  $u_z$  – drift velocity on the outer contour of the impeller,  $A$  – the inlet area of the pump impeller.

For the analysed Roto-Jet pump of the PCz 95.7 type, the kinematic shape number is approx. 2.1 and the nominal rotational speed is 8000 rpm. It should be noted that part of the work carried out under the project were numerical analyses of the pump, the exemplary calculation results of which are presented in Fig. 4.

The Roto-Jet pump uses a high-speed electro-spindle (PE3 12/2 model), produced by ELTE, whose basic operating parameters are given in Tab. 2. A photo and an assembly drawing of the designed and constructed pumping engine of the PCz 95.7 type are shown respectively in Figs. 5 and 6.

Table 2: Selected technical parameters of the PE3 12/2 electro-spindle manufactured by ELTE company [27].

Parametr	Value	Unit
Supply voltage	230/400	V
Current intensity	6.3/3.6	A
Frequency	200	Hz
Rotational speed	12 000	rpm
Shaft power	1.5	kW
Power factor ( $\cos \varphi$ )	0.79	–

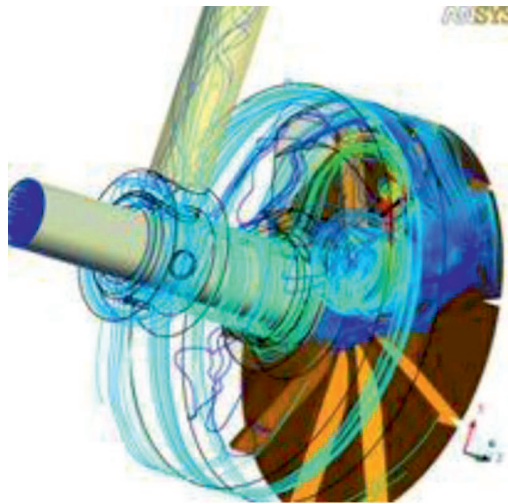


Figure 4: Exemplary results of numerical calculations of the Roto-Jet pump of the PCz 95.7 type [26].



Figure 5: Photo of the pumping engine with a Roto-Jet pump of the PCz 95.7 type [26].

The overall length of the pumping engine with a Roto-Jet pump is about 0.305 m. The pump (1) was connected using a jaw coupling with an elastic liner (3) to a high-speed electro-spindle (2). Then, both devices were mounted on the frame bearer (4). Selected structural components of the Roto-Jet pump are presented in Figs. 7 and 8. Due to aggressive environmental conditions that could cause corrosion, alloys of non-ferrous metals were used to construct the Roto-Jet pump.

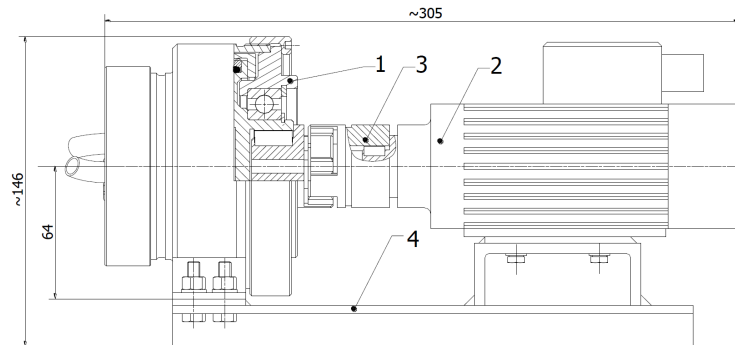


Figure 6: Assembly drawing showing the pumping engine of the PCz 95.7 type [26]:  
1 – Roto-Jet pump, 2 – engine, 3 – coupling, 4 – supporting frame.

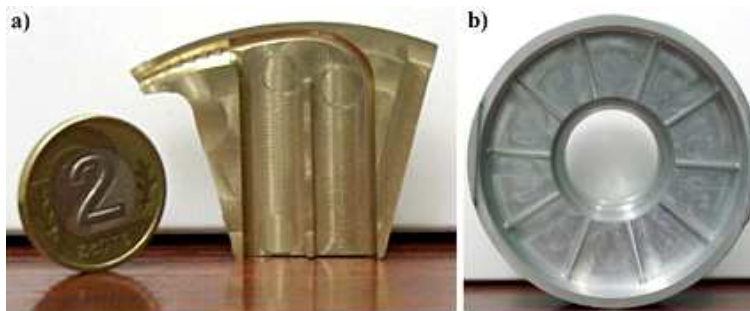


Figure 7: Photos of the bucket (a) and the drum's disk (b) of the rotor-jet pump of the PCz 95.7 type [26].



Figure 8: Photo showing elements of the bucket head of the Roto-Jet pump [26].

### 3 Research results

The research on a prototypical Roto-Jet pump (PCz 95.7 model) was conducted on the ORC system operating with and without regeneration. Load-

ing the pump was done using the expansion valve, which simulated operation of the expansion machine. The research work included measuring thermodynamic parameters of working fluids used in the ORC in order to illustrate the actual operating parameters of the installation.

First, the pump was subjected to research in the cycle without regeneration (Fig. 2). The temperature of the thermal oil at the evaporator inlet ranged from 117 °C to 135 °C, and at its outlet, it was in the range from 103 °C to 120 °C. The temperature of HFE7100 was in the range of 33–50 °C and 103–120 °C respectively at the evaporator's inlet and outlet, as shown in Fig. 9.

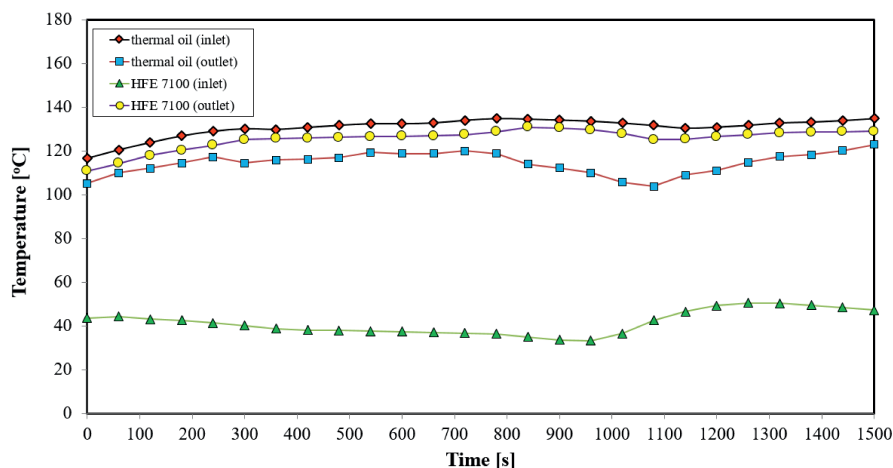


Figure 9: Temperature of the thermal oil and the HFE7100 fluid at the inlet and outlet of the evaporator operating in the ORC installation without regeneration *vs.* time.

The maximum temperature of HFE7100 at the evaporator outlet was 120 °C and was about 40 °C lower than the rated one, in order to protect the tested pump against high temperatures and its possible damage. Such a situation could have occurred because the system operated without a regenerative heat exchanger, and the throttle valve (expansion valve) can cause only a slight drop in temperature compared to expansion machines (e.g., turbines). After expansion, the HFE7100 fluid travelled towards the condenser, where at its inlet and outlet the temperature was in the range of 66–79 °C and 25–70 °C respectively, as shown in Fig. 10. The maximum temperature of the HFE7100 fluid at the condenser outlet was about 5 °C higher than the nominal operating temperature of the pump (65 °C). The

Roto-Jet pump enables safe operation in the system up to a temperature of approx.  $80^{\circ}\text{C}$  due to the maximum operating temperature of the seals used in the pump. The temperature of the cooling medium (glycol) was practically constant at the condenser's inlet (approx.  $18^{\circ}\text{C}$ ) and at its outlet, it varied from  $33^{\circ}\text{C}$  to  $70^{\circ}\text{C}$ , which resulted from the used method of regulating the load (throttling) of the Roto-Jet pump. In the initial stage of research, a high flow rate was maintained in order to prevent the excessive increase in the temperature of HFE7100 at the Roto-Jet pump's inlet, as presented in Fig. 11. The glycol flow rate varied from  $0.38\text{ kg/s}$  to  $0.84\text{ kg/s}$ . The research on the Roto-Jet pump was carried out virtually at a constant flow rate of the heating medium (thermal oil), and the flow changes were in the range of  $0.25\text{--}0.27\text{ kg/s}$ . The flow rate of the HFE7100 changed as the throttling level changed and was in the range of  $0.04\text{--}0.12\text{ kg/s}$ .

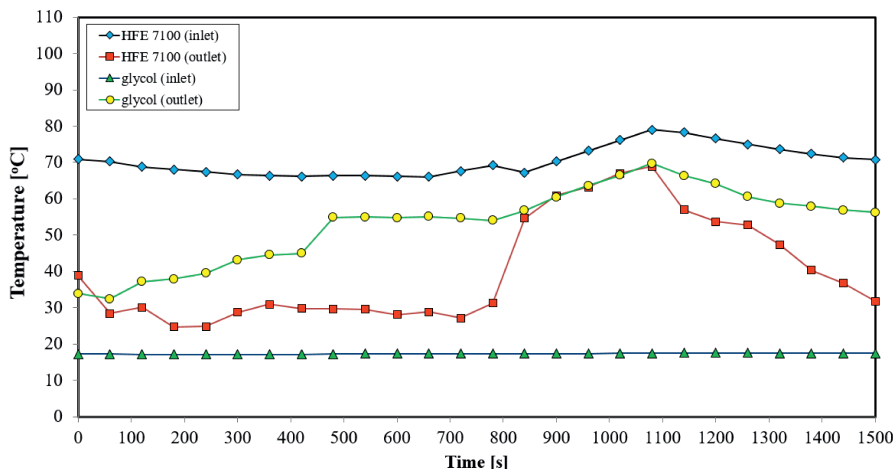


Figure 10: Temperature of the HFE7100 and glycol at the inlet and outlet of the condenser operating in the ORC installation without regeneration *vs.* time.

The pressure drop during the flow of HFE7100 through the evaporator (which is a plate heat exchanger) was in the range of  $9.15\text{--}10.0\text{ kPa}$ , and for the thermal oil, it changed from  $1.55\text{ kPa}$  to  $2.01\text{ kPa}$ , as shown in Fig. 12. As far as the condenser (which is also a plate heat exchanger) is concerned, the pressure drops on the HFE7100 side were in the range of  $0.01\text{--}1.9\text{ kPa}$  (Fig. 13). An increase in the resistance of flow was caused by a decrease in the glycol flow rate. This resulted in a perturbation in the heat removal from HFE7100 which led to a two-phase flow and a decline

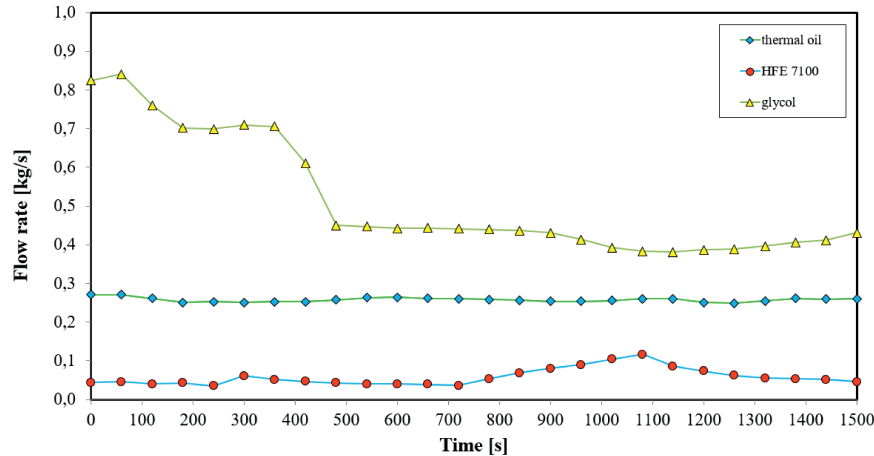


Figure 11: Flow rate of working fluids operating in the ORC installation without regeneration *vs.* time.

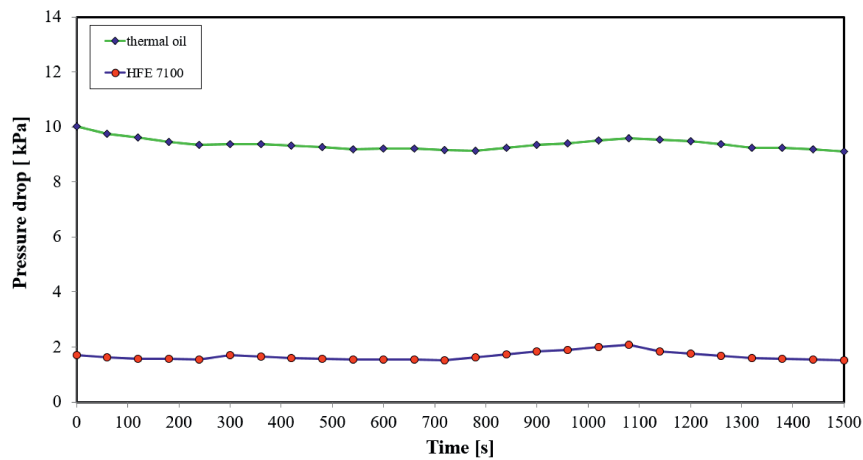


Figure 12: Pressure drop in the evaporator during the flow of the thermal oil and HFE7100 in the ORC installation without regeneration *vs.* time.

in the heat transfer coefficients causing an increase in the temperature of working fluids, which can be observed in Fig. 10. As far as the glycol side is concerned, the pressure drops were in the range of 0.45–1.11 kPa. Pressure drops in individual elements of the ORC installation were measured in order to determine their actual characteristics and verify the calculated flow resistances.

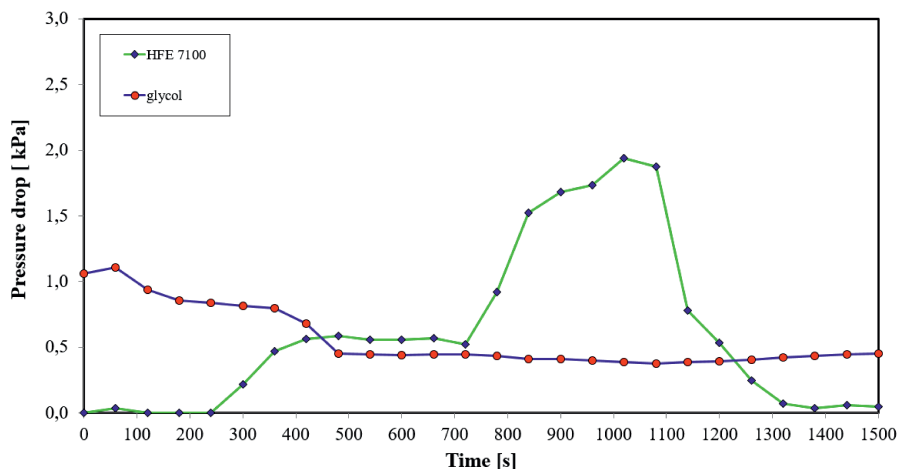


Figure 13: Pressure drop in the condenser during the flow of the HFE7100 and glycol in the ORC system without regeneration *vs.* time.

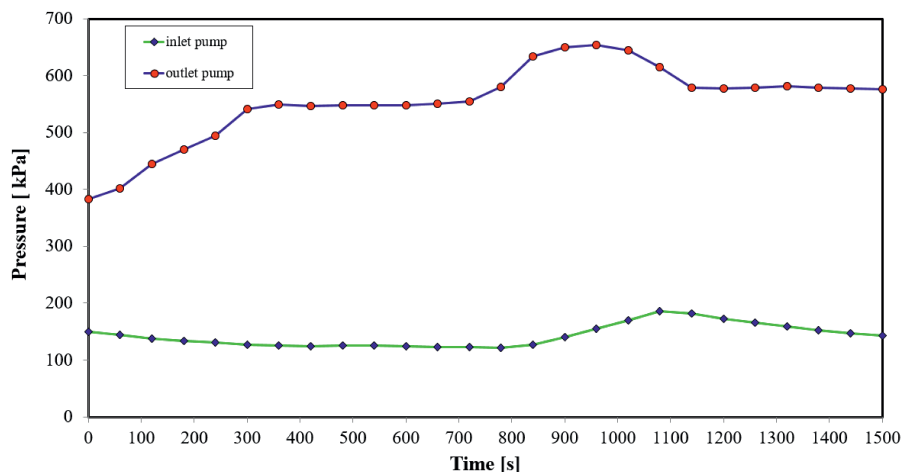


Figure 14: Relative pressure measured at the rotor-jet pump's inlet and outlet during its operation in the ORC system without regeneration *vs.* time.

Figure 14 demonstrates the pressure of the working fluid versus time, which was measured at the inlet and outlet of the Roto-Jet pump. The relative pressure of HFE7100 at the suction side of the pump was maintained during the measurements at a level of 1.22–1.85 kPa and resulted mainly from the glycol flow rate. Furthermore, the pressure at the delivery side of



the tested pump increased as the throttling level rose and it was in the range of 382.5–653.5 kPa. The maximum obtained pressure of the working medium was almost 50% lower than the pressure required in the ORC system. Thus, at the maximum pressure value, the flow rate of HFE7100 was about 0.08 kg/s, while the required level is 0.17 kg/s.

Based on the results of the measurements that are shown above, the characteristics of the Roto-Jet pump were determined (Fig. 15). As we can see, the maximum delivery head is about 45 m at the flow rate of the working fluid of approx. 0.08 kg/s.

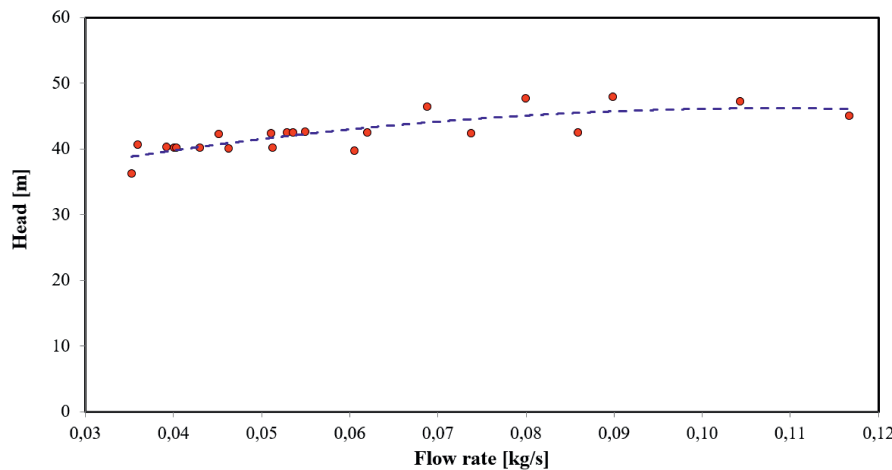


Figure 15: The delivery head of the rotor-jet pump *vs.* flow rate of the HFE7100 (measured during the operation in the ORC system without regeneration).

Figure 16 presents the saturation curve of the working fluid and experimental results obtained during the testing of the Roto-Jet pump. Among helpful tips on how to guarantee safe operation of an expansion turbomachine (e.g., a turbine) are the following ones: appropriate pressure and flow rate of the working fluid must be provided as well as the appropriate degree of dryness of the vapor is required. Vapor directed to the stator should be dry ( $x = 1$ ), and preferably superheated ( $x > 1$ ), which protects against erosion and damage to the turbine's flow system.

The saturated vapor of HFE7100 was obtained in the pressure range of 310–380 kPa, and superheated vapor occurred when the pressure was higher than 380 kPa. The temperature of the thermal oil and HFE7100 medium versus time, measured at the inlet and outlet of the evaporator

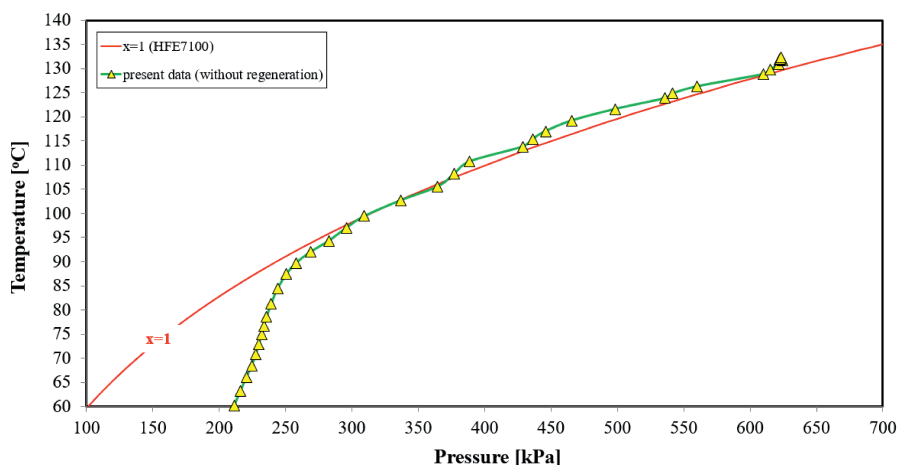


Figure 16: HFE7100 saturation curve and experimental results obtained during testing of the rotor-jet pump operating in the ORC system without regeneration.

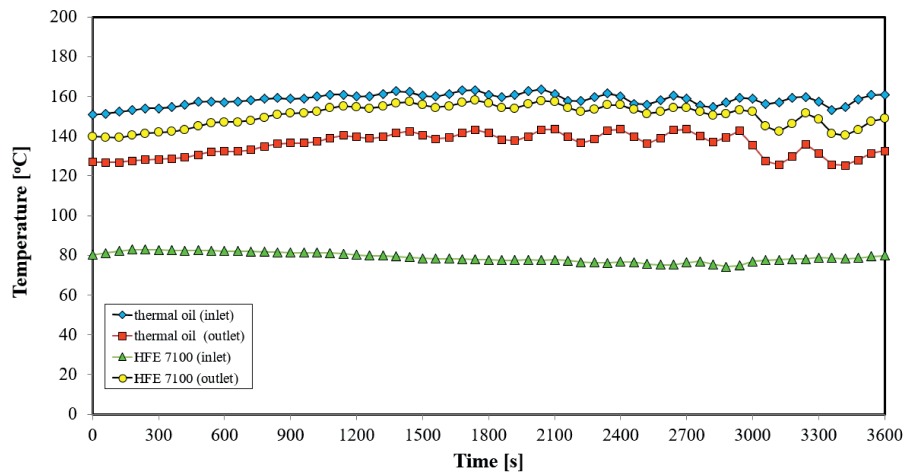


Figure 17: Temperature of thermal oil and HFE7100 at the inlet and outlet of the evaporator operating in the ORC installation with regeneration *vs.* time.

operating in the ORC installation with regeneration, is shown in Fig. 17.

The temperature of the thermal oil at the evaporator inlet ranged from  $150.8^{\circ}\text{C}$  to  $163.5^{\circ}\text{C}$ , and at its outlet, it was in the range from  $125.7^{\circ}\text{C}$  to  $142.8^{\circ}\text{C}$ . The temperature of HFE7100 at the evaporator inlet was about  $80^{\circ}\text{C}$ , and at its outlet, it was in the range from  $138.8^{\circ}\text{C}$  to  $157.8^{\circ}\text{C}$ .

The nominal temperature of the working fluid at the evaporator outlet is approx. 160 °C.

Looking at Fig. 18, one can see that the temperature of the HFE7100 fluid was in the ranges of 73.4–79.4 °C and 25.1–49.1 °C respectively at the condenser's inlet and outlet. The temperature of glycol at the condenser inlet was at a level of 17–20 °C, and at its outlet, it varied from 24.6 °C to 52.9 °C.

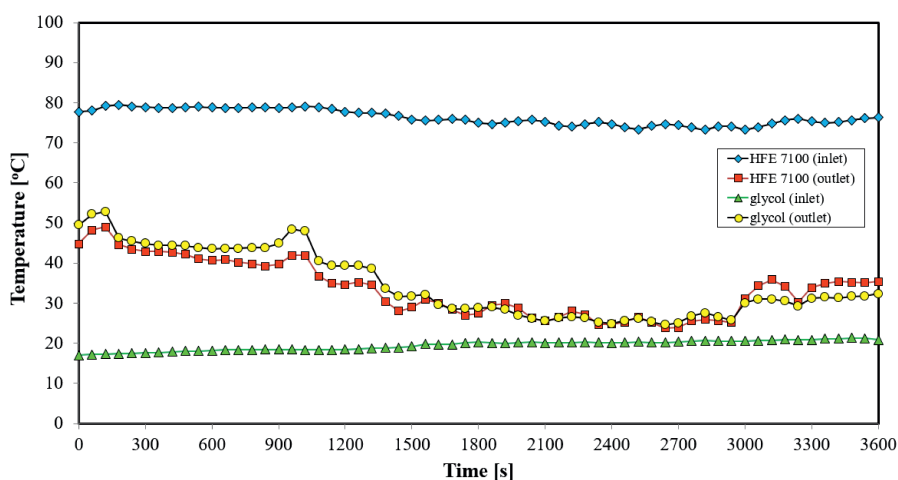


Figure 18: Temperature of HFE7100 and glycol at the inlet and outlet of the condenser operating in the ORC installation with regeneration *vs.* time.

The temperature of liquid at the regenerator inlet ranged from 31 °C to 49.1 °C, and at its outlet, it varied from 74.8 °C to 83 °C, as shown in Fig. 19. And at the vapor side, the temperature of HFE7100 was in the ranges of 77–86.6 °C and 73.3–79.5 °C, respectively at the regenerator's inlet and outlet.

Due to the high ambient temperature (about 38 °C) of the cooling tower and the need to ensure adequate heat removal conditions, it was necessary to increase the glycol flow rate to 4.63 kg/s, as shown in Fig. 20. Under such operating conditions of the ORC system, the flow rate of HFE7100 and of thermal oil was in the ranges of 0.06–0.18 kg/s and 0.22–0.25 kg/s, respectively.

An increase in the glycol flow rate caused that the pressure drop of the thermal oil in the evaporator decreased from approx. 9 kPa to 7.8 kPa, as shown in Fig. 21. However, the pressure drop on the HFE7100 side was in

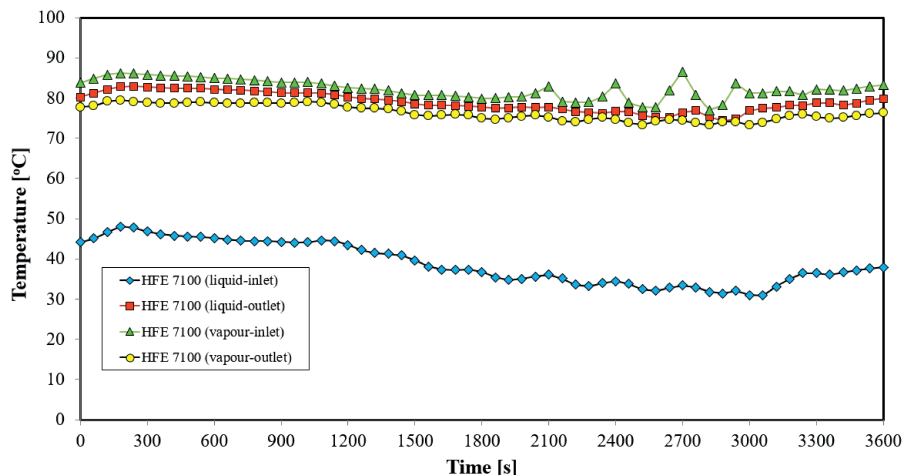


Figure 19: Temperature of the HFE7100 medium measured at the inlet and outlet of the regenerator during its operation in the ORC system with regeneration *vs.* time.

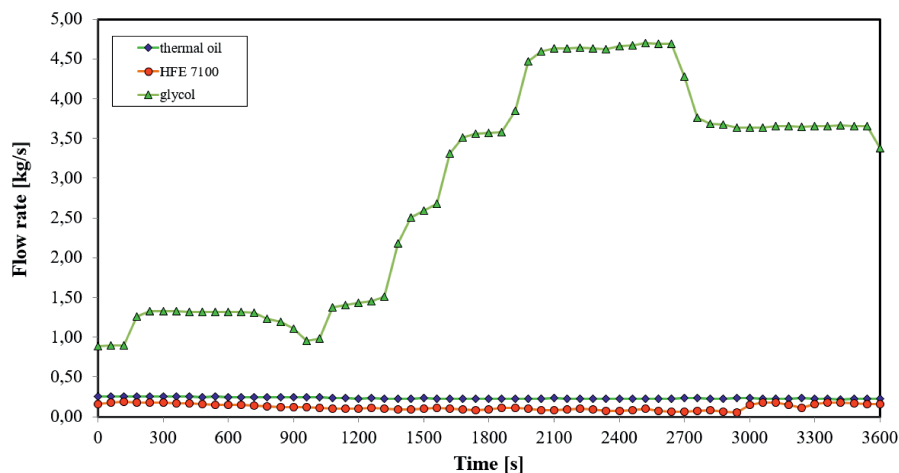


Figure 20: Flow rate of working fluids operating in the ORC installation with regeneration *vs.* time.

the range from 1.6 kPa to 4.2 kPa and decreased as the cooling power of the cooling tower increased.

Moreover, an increase in the glycol flow rate caused a significant increase in the resistance of flow in the cooling installation (in the condenser). It

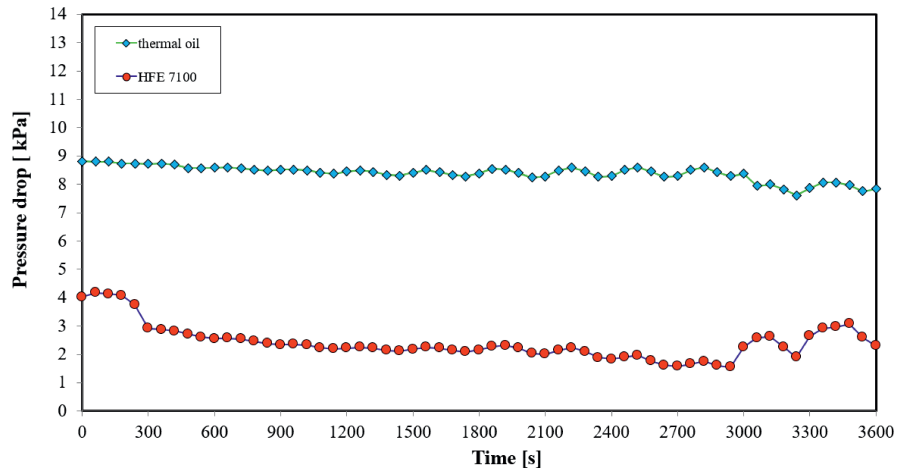


Figure 21: Pressure drop in the evaporator during the flow of the thermal oil and HFE7100 in the ORC system with regeneration *vs.* time.

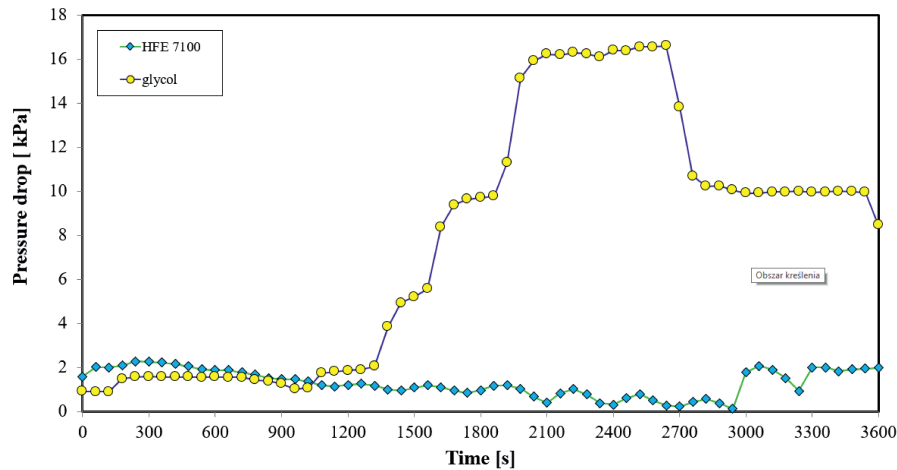


Figure 22: Pressure drop in the condenser during the flow of the glycol and HFE7100 in the ORC system with regeneration *vs.* time.

was observed that the pressure drop in the condenser increased from approx. 1.5 kPa to approx. 16.6 kPa (Fig. 22).

In the system with regeneration, additional pressure drops in the installation were caused by the regenerator (shell-and-tube heat exchanger), as shown in Fig. 23.

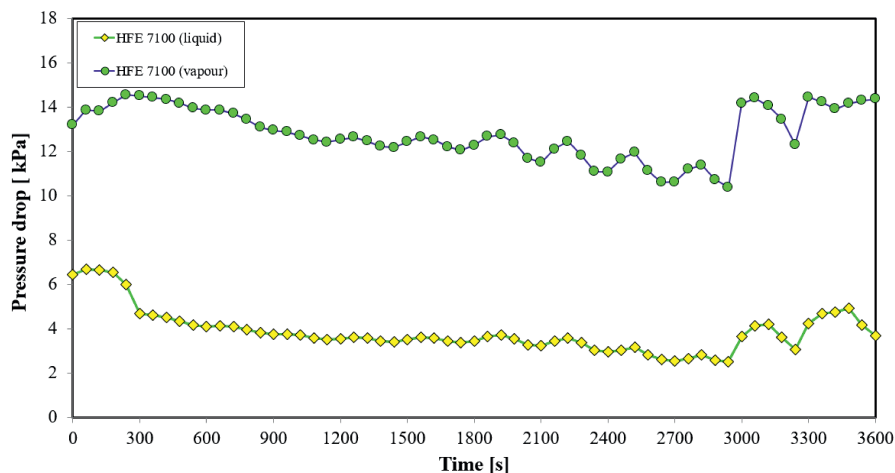


Figure 23: Pressure drop in a shell-and-tube heat exchanger (regenerator) during the flow of HFE7100 in the ORC system with regeneration *vs.* time.

HFE7100 generated pressure drops ranging from 10.4 kPa to 14.6 kPa during its flow through the regenerator's tubes, and HFE7100 in the form of vapor caused pressure drops in the range of 2.5–6.7 kPa when it flowed through the shell of heat exchanger.

Under the obtained operating conditions of the ORC system, the maximum pressure of the tested Roto-Jet pump was around 1.220 kPa at a suction pressure of about 175 kPa, as presented in Fig. 24.

However, at the required flow rate level of the HFE7100 (namely at 0.17 kg/s), the delivery head of the Roto-Jet pump is approximately 85 m (Fig. 25), which is 23 m lower than the value required for the proper functioning of the vapor turbine to be constructed.

The next very important issue is to provide the vapor of proper parameters to the turbine inlet. As can be seen on the graph shown in Fig. 26, superheated vapor did not occur in the entire operating range of the Roto-Jet pump. The absence of superheated vapor was probably caused by excessive supercooling of the working fluid vapor inside the regenerator, which means that the ORC system must have operated under the conditions of the wet vapor ( $0 < x < 1$ ). It should be noted that the HFE7100 vapor moisture level was not measured during the experimental research. However, the above statement is based on the observation that there was an approximately 2-fold increase in the resistance of flow in the evaporator of the ORC system with regeneration (see Fig. 21, which shows that the

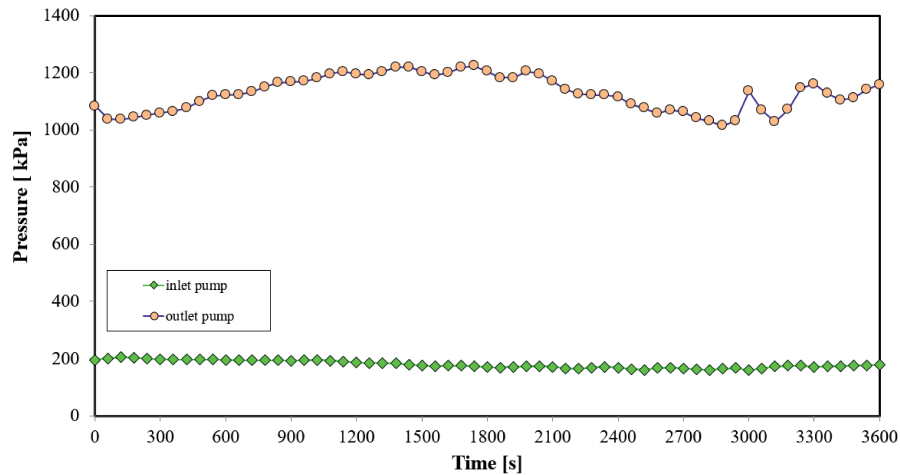


Figure 24: Relative pressure measured at the Rotor-Jet pump's inlet and outlet during its operation in the ORC system with regeneration *vs.* time.

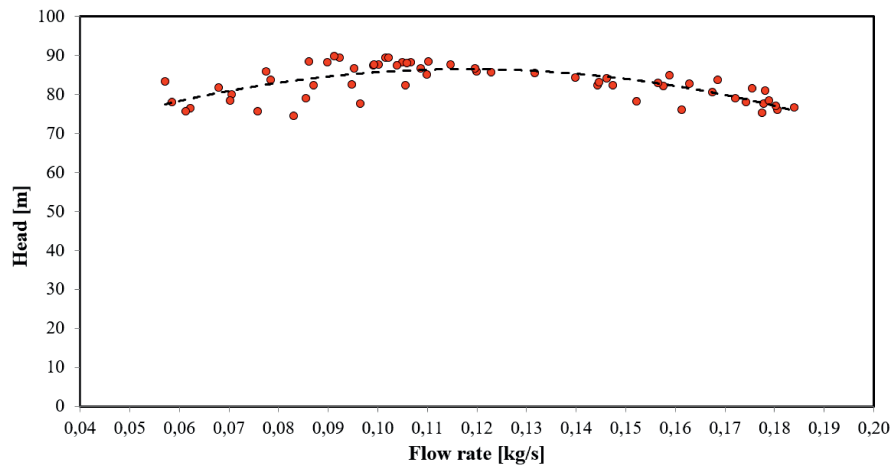


Figure 25: Delivery head of the Roto-Jet pump *vs.* flow rate of HFE7100 (measured during the operation in the ORC system with regeneration).

maximum pressure of HFE7100 was approx. 4.2 kPa) as compared to the ORC system with no regeneration (see Fig. 12, where the maximum pressure was approx. 2.01 kPa).

Furthermore, during the research on the organic Rankine cycle with regeneration, excessive noise and vibration levels of the pump were ob-

served in the vicinity of the coupling that connects it with the high-speed electro-spindle.

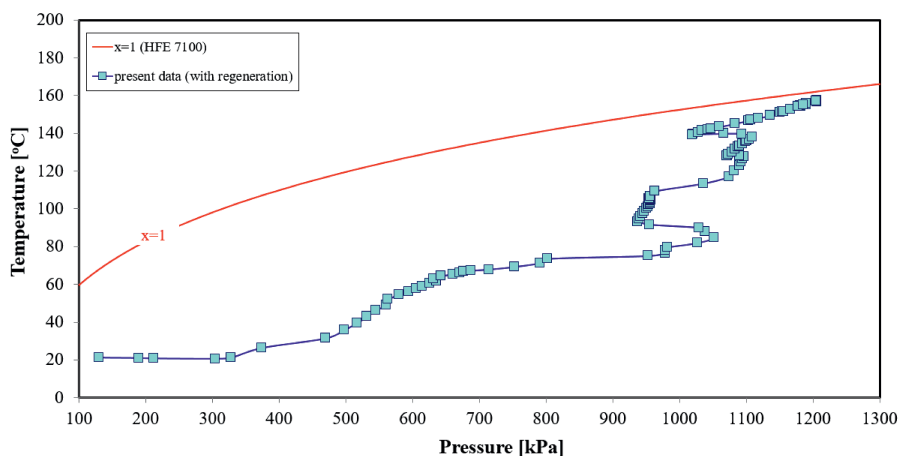


Figure 26: HFE7100 saturation curve and experimental results obtained during testing of the Roto-Jet pump operating in the ORC system with regeneration.

## 4 Summary

The paper presents results of the research on a prototypical Roto-Jet pump of the PCz 95.7 type, which operated in the ORC system with a low-boiling fluid (HFE7100). The research was conducted using the organic Rankine cycle both with and without regeneration. Thermal and flow characteristics of the most important components of the micro-cogeneration power plant as well as characteristics of the Roto-Jet pump were presented. It was found that in the ORC without regeneration, the maximum pressure generated by the Roto-Jet pump was around 653 kPa at the HFE7100 flow rate of 0.08 kg/s. In the cycle with regeneration, the maximum pressure was approx. 1220 kPa at a flow rate of HFE7100 of approx. 0.11 kg/s. During the research on the cycle with regeneration, excessive noise and vibration levels of the pump were noticed in the vicinity of the coupling that connects it with the high-speed electro-spindle. Based on the carried out research, the authors plan to modernize the pumping engine in the immediate future.

On the basis of experience from the research and operation tests conducted so far, it is clear that a new supply system and a new outlet of the



Roto-Jet pump of the PCz 95.7 type should be developed, which could improve its energy performance. The planned changes are aimed at enhancing the efficiency of the pump (including the increase in its delivery head) by significantly increasing the volumetric flow rate both at the inlet and outlet as well as a better positioning of the stream.

In order to improve the manufacturing technology of the rotating system, its construction should be modified. This can be done using a rotor disk embedded in the rotary drum body as well as applying a different division of the drum. Such a solution will significantly simplify the process of manufacturing the grids of blades. What is more, both the method of affixing of the bucket head and the rinsing system of the end-face mechanical seal should be altered.

Received 19 November 2018

## References

- [1] LEI B., WANG J.-F., WU Y.-T., MA CH.-F., WANG W., ZHANG L., LI J.-Y.: *Experimental study and theoretical analysis of a Roto-Jet pump in small scale organic Rankine cycles*. *Energ. Convers. Manage.* **111**(2016), 198–204.
- [2] QUOILIN S., BROEK M.V.D., DECLAYE S., DEWALLEF P., LEMORT V.: *Techno-economic survey of Organic Rankine Cycle (ORC) systems*. *Renew. Sust. Energ. Rev.* **22**(2013), 168–18.
- [3] MIAO Z., XU J., YANG X., ZOU J.: *Operation and performance of a low temperature organic Rankine cycle*. *Appl. Therm. Eng.* **75**(2015), 1065–1075.
- [4] BORSUKIEWICZ-GOZDUR A.: *Pumping work in the organic Rankine cycle*. *Appl. Therm. Eng.* **51**(1-2)(2013), 781–786.
- [5] KACZMARCZYK T.Z., ŻYWICA G., IHNATOWICZ E.: *Experimental investigation on a rotodynamic pump operating in the cogeneration system with a low-boiling working medium*. *Trans. Inst. Fluid-Flow Mach.* **134**(2016), 63–87.
- [6] MEYER J., DARÓCZY L., THÉVENIN D.: *Shape optimization of the pick-up tube in a Pitot-tube jet pump*. *J. Fluids Eng.* **139**(2017), 021103-1/ 021103-11.
- [7] MEYER J., DARÓCZY L., THÉVENIN D.: *New design approach for Pitot-tube jet pump*. In: *Proc. ASME Turbo Expo 2014: Turbine Technical Conf. Expos. GT2014*, June 16–20, 2014 Düsseldorf, 1–8.
- [8] PN-EN ISO 5199:2004 standard – Technical requirements for centrifugal pumps – Class II (in Polish).
- [9] ISO 10816-3:2009 standard – Mechanical vibration – Evaluation of machine vibration by measurements on non-rotating parts – Pt. 3: Industrial machines with nominal power above 15 kW and nominal speeds between 120 rpm and 15 000 rpm when measured in situ.

- [10] ISO 10816-7:2009 standard – Mechanical vibration – Evaluation of machine vibration by measurements on non-rotating parts – Pt. 7: Rotodynamic pumps for industrial applications, including measurements on rotating shafts.
- [11] ANSI/API 610 standard – Centrifugal pumps for petroleum, petrochemical and natural gas industries.
- [12] LORENZ W., JANCZAK M.: *Successes and failures in the CFD flow modeling work with respect to low specific speed multistage centrifugal pumps*, *Mechanik* **3**(2016), 141–145.
- [13] LORENZ W., JANCZAK M.: *Analysis of the reasons of double suction centrifugal pump's failure*, *Mechanik*, 11, 1084–1087, 2017.
- [14] BŁASZCZYK A., PAPIERSKI A., SUSIK M.: *New design method for the formed suction intake in axial-flow pumps with a vertical axis*. *Mechanics Mechanical Eng.*, **20**(2016), 4, 553–568.
- [15] PLUTECKI W.: *Bucket pumps. Construction, parameters, application*. *Pompy i Pompowanie* **2**(2006), 43–45 (in Polish).
- [16] KACZMARCZYK T.Z., ŻYWICA G., IHNATOWICZ E.: *Experimental research on the domestic ORC micro power plant with a commercial biomass boiler*. In: Proc. 3rd Int. Conf. on Energy and Environmental Protection, E3S Web of Conferences 46, 00021, 2018. <https://doi.org/10.1051/e3sconf/20184600021>
- [17] OSBORN S.: *The Roto-Jet pump: 25 Years New*. *World Pumps* **363**(1996), 32–36.
- [18] HUANG S., SU X., YANG F., GUO J.: *Numerical simulation of 3D unsteady flow in Roto-Jet pump by dynamic mesh technique*. *Prog. Comput. Fluid Dyn.* **15**(2015), 4, 265–267.
- [19] WANG C., ZHAO C.L., ZHANG T.F., LIU D.: *The numerical simulation of full flow field of Roto-Jet pump and analysis of energy losses*. *Adv. Mat. Res.* **562**(2012), 1369–1372.
- [20] LORENZ W.: *Carried out laboratory tests and validation of the special type centrifugal pump*. *Mechanik* **10**(2016), 1286–1289.
- [21] LORENTZ W., PLUTECKI J.: *Bucket pump with the bucket*. National patent PL 224914 B1, 2017, Feb. 28.
- [22] LORENTZ W., PLUTECKI J.: *Drain pipe*. National patent PL 224916 B1, 2017, Feb. 28.
- [23] ANGLE T.L., SHAW J.G., CUMMINS S., TURNER M.: *A new unique high-pressure pump system*. In: Proc. 22nd Int. Pump Users Symp., Houston 2005, 23–33.
- [24] KOMAKI K., KANEMOTO T., SAGARA K., UMEKAGE T.: *Effect of the collector tube profile on Pitot pump performances*. In: Proc.: 6th Int. Conf. on Pumps and Fans with Compressors and Wind Turbines, IOP Conf. Ser.: Mat.Sci. Eng. **52**(2013), 032021–032026.
- [25] ZHU Y., KANG C., MAO N.: *Influence of the collector and the inner guide vane on Roto-Jet pump performance*. *Int. J. Fluid Dyn.* **4**(2016), 3, 33–42.
- [26] KANIECKI M., HENKE A., KRZEMIANOWSKI Z.: *Pump aggregates in application to ORC micro cogeneration power plant*. Wydawnictwo IMP PAN, Gdańsk 2013 (in Polish).
- [27] Catalogue card of the PE3 12/2 electro-spindle manufactured by ELT.